Towards a Mobile Mapping Robot for Underground Mines

Conference Paper · November 2014

CITATIONS
50

4 authors, including:

Tobias Neumann
FH Aachen
7 PUBLICATIONS **84** CITATIONS
SEE PROFILE

Alexander Ferrein
FH Aachen
147 PUBLICATIONS **1,621** CITATIONS
SEE PROFILE

Stephan Kallweit
FH Aachen
45 PUBLICATIONS **327** CITATIONS
SEE PROFILE

Towards a Mobile Mapping Robot for Underground Mines

Tobias Neumann*, Alexander Ferrein*†, Stephan Kallweit* and Ingrid Scholl*
*Mobile Autonomous Systems & Cognitive Robotics Institute
FH Aachen University of Applied Sciences, Aachen, Germany
†Centre of AI Research, UKZN and CSIR, South Africa
Email: tobias.neumann@alumni.fh-aachen.de, {ferrein, kallweit, scholl}@fh-aachen.de

***Abstract*—In recent years a lot of research has focussed on introducing mobile robots into production scenarios. Mobile robots are already deployed in flexible supply chain applications, moving the parts, which are to be processed next, to the right machines on time. In mining industries, particularly when operating underground, load-haul-dump vehicles are deployed under much harder environmental conditions compared to warehouses. In both cases, accurate environment maps help to localize the vehicles and robots. In this paper, we describe our robot platform which will be deployed in underground mapping scenarios. For generating accurate 3D environment maps, we equipped the robot with a Velodyne LiDAR and developed a tilt unit which allows the LiDAR to be tilted between 0° and 90°. We describe the hardware design of the tilt unit and the control software of the robot which runs under the Robot Operating System. For acquiring data, the tilting LiDAR can be run in two modes: stop-and-go scanning and continuous scanning. We compare both modes and report on our first experiments where we acquired data from a $2.4\,$km stretch of a motorway tunnel.**

I. Introduction

In recent years a lot of research has focussed on introducing mobile robots into production scenarios. Mobile robots are already deployed in flexible supply chain applications, moving the parts, which are to be processed next, to the right machines on time. The keyword for this future production scenario is *cyber-physical systems* [1], [2]. For warehouse scenarios there are already some very successful examples of deploying mobile robots for logistics tasks. For instance, Amazon deploys KIVA robots for their commissioning tasks in their warehouses on a large scale [3]. In mining industries, particularly when operating underground, the environmental conditions are much harder than in warehouses. This might be a reason why autonomous vehicles have not yet been deployed to the same extent here. Notwithstanding, visions of fully automated (underground) operations exist such as the Rio Tinto "Mine of the future" project [4]. Before this vision can become reality, more research and development is required in the relevant areas of mobile robotics research. A number of approaches focus on navigation and collision avoidance, e.g. [5]–[7]. These approaches yield results for automating open-pit mines with load-haul-dump (LHD) vehicles or autonomous container terminal robots [8]. The mobile systems are deployed in large numbers in productive operation.

Apart from such large scale applications of automated LHD vehicles and container terminal robots, automation in mining focusses also on improving the miner's safety on-site. If a robot device can do some of the dangerous jobs of a miner, the miner can concentrate on other important objectives. The question of whether robots can improve the safety of a miner, can be positively answered, for instance, in the case of South African deep mining [9]. In [10], a robot device that can detect loose rocks in the hanging-wall is presented. In [11], some existing aerial as well as ground vehicles that could be helpful in rescue missions for mining disasters are discussed. An important aspect of automating mines and LHD vehicles is to have an environment map of a mine at hand that can be used for the autonomous vehicles to localize themselves. A precise map of the mine is also helpful for the mine operators to better plan their activities. The map of the mine that is acquired by the mobile mapping robot can then, in turn, be used by other LHD vehicles to localize themselves.

In this paper, we present our underground mapping robot Barney. We equipped the robot with a Velodyne 64 LiDAR, which was also deployed in the DARPA Urban Challenge [12]. The device yields up to 1.3 million points per second with a vertical field of view (VFOV) of about 26.8° at about 0.5° resolution and a horizontal field of view (HFOV) of 360° at 0.09° resolution. In order to use this sensor for mapping applications, we developed a tilt unit that is able to tilt the sensor vertically between 0° and 90°. As tilting the sensor is quite challenging due to its weight of $15\,$kg, we briefly discuss the mechanical design of the tilt unit. For acquiring a complete scan at a certain position, the tilt unit takes a sweep between 0° and 90°, integrating single point clouds taken at different angles into a local map at the robot's current position. The robot does not move while scanning. There are two scanning possibilities: (a) stop-and-go acquisition and (b) continuous acquisition. In the former case, the tilt unit stops at certain predefined angles, the sensor acquires a point cloud and moves to the next angle. In the latter case, the tilt unit tilts between 0° and 90° while continuously acquiring point clouds. With continuous scanning, much denser local maps can be acquired as more point clouds are integrated into the map. Outliers and sensor noise are easier to average out and the maps computed from denser point clouds will be more accurate. For obtaining the tilt angle and therefore for registering point clouds at the correct pose, we make use of an additional IMU which is attached to the tilt unit. This way, we can register point clouds

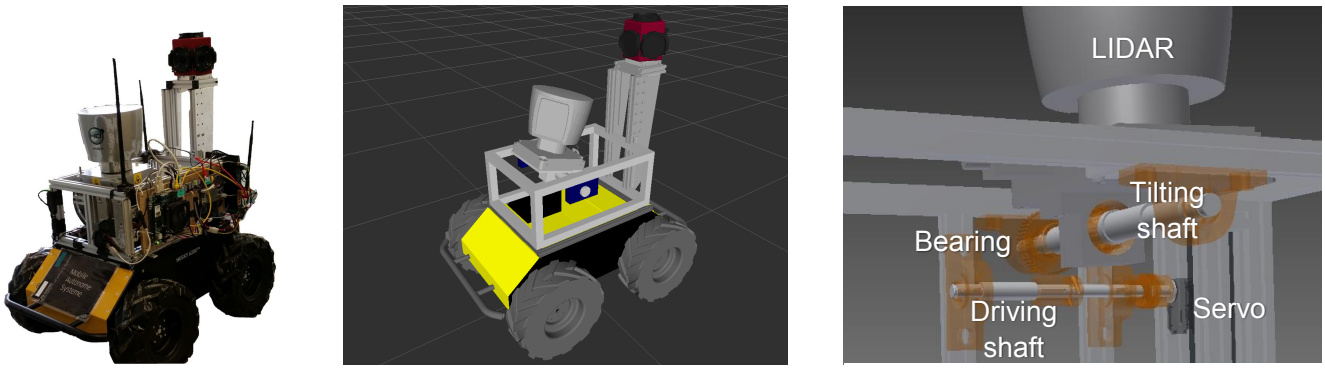

(a) The underground mapping robot Barney.

(b) The URDF simulation model of Barney for the Gazebo simulator.

(c) Details of the tilt unit mechanism.

Figure 1. The Underground Mapping Robot Barney.

in an easy way without using sophisticated but computationally expensive algorithms such as iterative closest point algorithms (ICP) [13]. In our first experiments, we acquired data from a 2.4 km stretch of a motorway tunnel in Austria.

The rest of the paper is organized as follows. In the next section, we review some related work of underground mine mapping, before we outline the robot platform and the tilting LiDAR device. We then present some of our first experimental data from the motorway tunnel and compare continuous and stop-and-go scanning. We conclude with a discussion and an outlook to future work.

II. Related Work

The related work in this section reviews, for one, work from mapping underground mines with autonomous robots; for another, we review the state of the art of unmanned ground vehicle deployment in underground mines. The probably most related work in the area of 3D tunnel mapping is presented in [14], [15]. There, Thrun et al. present an approach for mapping inactive or abandoned mines in 3D in an accurate way using simultaneous localization and mapping (SLAM). They use the rugged terrain vehicle Groundhog and a Pioneer2 for their experiments, which are equipped with two laser range finders (LRF). One LRF is aligned along the ground plane of the robot, the other one is mounted orthogonally to that plane pointing towards the ceiling. They map the mine in 2D and use a 2D scan matching approach to estimate the displacement and orientation difference between consecutive scans. Due to loops in the environment, the global map cannot be constructed from the scan matching algorithm. For this purpose, they use a version of the iterative closest point algorithm for the loop closure. In a post-processing step, a 3D model of the 2D poses, together with the range scans which point towards the ceiling, is reconstructed. Another closely related work to the 3D mapping problem in rugged terrains is described in [16], [17]. In fact, for approaching the 6D SLAM problem, they improved scan registration done by ICP by calculating heuristic initial estimates for ICP based on a 6D odometry extrapolation. If loop closure is possible (it is detected that the robot came across the same position again), the error is distributed to improve the alignment of the scans. The initial estimates for ICP are computed by a coarse-to-fine strategy in an octree representation, where first the displacement and rotation of two scans are estimated on a coarse octree resolution; the resolution is stepwise refined, and with it the estimate as well. For run-time optimization on the robot, they deploy KD-trees for searching 3D points in their point clouds. Besides mapping experiments in indoor and outdoor environments and testing the method in RoboCup Rescue scenarios, they also mapped the Kvarntorp mine near Örebrö in Sweden with their robot platform Kurt3D. Kurt was able to map the mine environment in 3D with high accuracy. Another recent paper relevant to our work is [19]. There, an automatic calibration routine for a LiDAR and a camera system is presented and also tested in an open-pit mine environment. For combining camera data with data from a Velodyne the authors describe the problem that ordinary Velodyne data (from a not-tilted sensor) are too spare such that for 95% of the camera data there are no depth information. Besides those papers already mentioned in the introduction about LHD vehicles and mining safety [5]–[11], Morris et al. [18] discuss the basics of void entry, mobility, sensing, navigation, modelling, and subterranean operations. In particular, they show the huge advantages for moving through underground voids that preclude human access. Instead of classical SLAM approaches, they use an incremental scan matching for short-term position estimation and a topological SLAM for global localization.

III. The Underground Mapping Robot Barney

A. The Underground Robot Platform

Our underground robot Barney (Fig. 1(a)) is based on the Clearpath Husky robot platform, which is a four-wheeled differential drive robot base. The robot has external dimensions of 990 mm × 670 mm × 390 mm, weighs 50 kg and has an additional payload of 75 kg. With its ground clearance of about 130 mm it is well-suited for (limited) rugged-terrain deployment which we aim for with our mapping application.

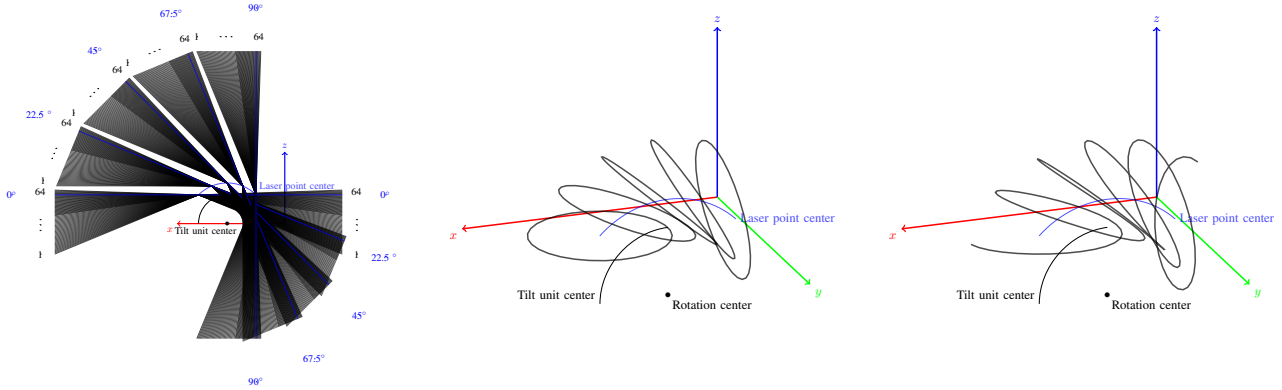

(a) The vertical field of view with scans taken at 0°, 22.5°, 45°, 67.5° and 90°

(b) Circular movement of the sensor head during stop-and-go scanning.

(c) The helical movement of the sensor head in the continuous mode.

Figure 2. The field of view of the Velodyne LiDAR on the tilt unit.

As far as built-in sensor equipment, it only comes with wheel encoders. The system is fully integrated into the Robot Operating System, (ROS) [20]. To increase the accuracy of odometry measurements, we equipped the robot with an XSENS MTi-300 attitude heading reference system (AHRS). To be able to acquire dense 3D maps of the mining environment, we developed a tilt unit for the Velodyne HDL-64E S2 LiDAR which is capable of tilting the LiDAR between 0° and 90°. To obtain the tilt angle of the tilt unit, we installed an additional XSENS MTi-10 IMU on the mounting platform. In Fig. 1(a) one can also spot a Point Grey Ladybug 5 spherical camera as an additional sensor on our platform. In our future work, we will map images from the spherical camera to the registered point clouds in order to generate coloured point clouds. In the next section, we describe the hardware and the control software of the tilt unit in greater detail.

B. The Tilting LiDAR System

1) Hardware Design: There are several ways of designing tilt units for laser range finders. A common way is the use of a standard servo where a mounting platform is driven directly by rotating around the horizontal axis. This works fine for small laser scanning units with low weights. The deployed Velodyne HDL-64E with a mass of 15 kg would require quite a large drive unit for tilting it that way. As an alternative, one could use one of the following mechanical designs: (a) four bar linkage, (b) cam and follower or (c) worm gears. The standard planar four bar linkage is suitable for transforming a rotational movement of a driving motor to a large choice of planar trajectories. It is often the most efficient and simplest way of generating the desired motion. The drawback of using it for a tilt mechanism is the non-constant speed ratio: for a desired constant angular tilt velocity, the drive unit would need a fine adjustable servo drive to compensate the non-constant gear ratio. What is more, the size of a four bar linkage is often larger than a cam and follower design providing the same trajectory. One drawback here is that the cam needs to be manufactured with high accuracy. Dynamic loads such as momenta and forces can also be critical: in a planar arrangement, cam and follower are interacting in a line; this leads to higher stresses compared to a four bar linkage design. Worm gears can have quite a high constant gear ratio and can cope with high loads and momenta. Another benefit is that they are self-locking, so that the driving servo motor can be switched off without risking a harmful movement of the LIDAR system. For designing the gear system, an optimal rotation point w.r.t. the different lengths of the lever arm of the weight forces that occur during a tilt motion can be calculated.

As a driving motor, a Dynamixel MX-106R is used providing up to 10 Nm torque, a resolution of 4096 increments per revolution and known ROS support. A metal bellow clutch is used for connecting the MX-106R to the spring-loaded drive shaft. Diaphragm springs were used to reduce the gear backlash of the combination of the two worm gears having a gear ratio of 46:1. The hysteresis can be compensated by only driving the tilt mechanism in one direction. Fig. 1(c) shows some of the details of the design. The design was validated in simulations (with Autodesk Inventor) to get correct peak momenta and their distributions. The peak value for the drive torque is less than $\sim$2 Nm , far less than the limit of the MX-106R. A similar analysis was done for the tilt shaft. The time-dependent torque of the tilt shaft has a maximum value of $\sim$ 38 Nm .

2) Controlling the Tilt Unit with ROS: Similar as with the approaches outlined in Section II, we need to register single scans and compute a local map at the robot's current position. The Velodyne LiDAR has a field of view of 26.8°. To acquire a complete point cloud with a total vertical field of view of 116.8° (90 degrees plus the VFOV of the LiDAR), we need to combine several single measurements. Fig. 2(a) shows a vertical cross-section at the y-axis of the field of view.

For scanning and registering the data with the tilt unit, we have two different options: (a) stop-and-go scanning and (b) continuous scanning. The stop-and-go scanning works as follows: between 0° and 90° we stop the tilt unit motors

Figure 3. Mapping the Plabutschtunnel in Graz, Austria, with the robot Barney.

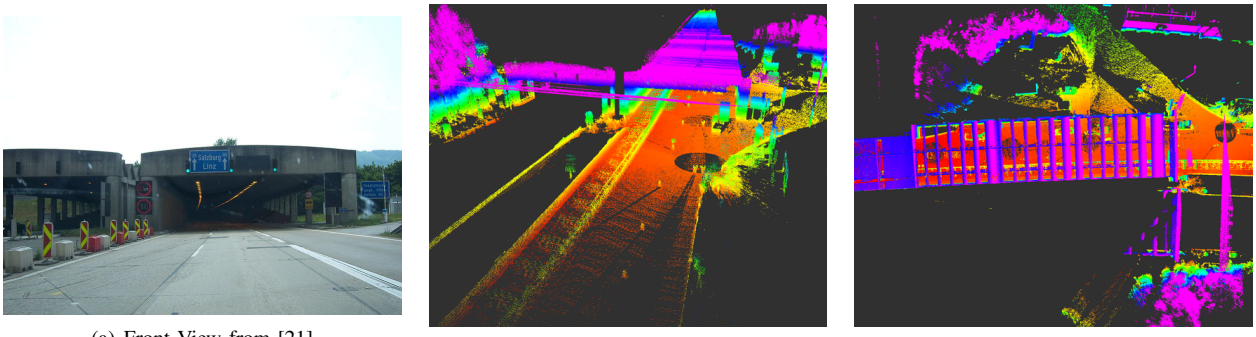

(a) Front View from [21] (b) Front view (c) Top view

Figure 4. The tunnel portal.

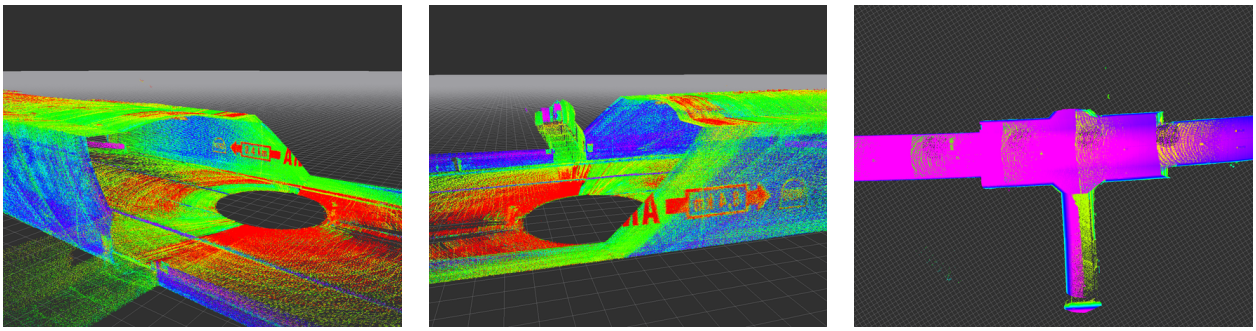

(a) Side view (intensity measurements) (b) Reverse angle (intensity measurements) (c) Top view (height measurements)

Figure 5. Emergency bay 1.8 km inside the tunnel.

usually in 5° steps and capture one 360° scan of the Velodyne. We developed our own ROS driver for the Velodyne (basically we wrapped the HDL driver from the *Point Cloud Library* (PCL) [22]) as we experienced problems with our version of the Velodyne and the standard Velodyne driver that comes with ROS. The scanning motion is shown in Fig. 2(b). At each angle position, the captured point cloud is added to the local map at the robot's current position. The motion of a continuous scan between 0° and 90° results in a helical motion of the sensor head as shown in Fig. 2(c). The challenge when scanning in the continuous mode is to associate the raw data stream from the LiDAR with the correct rotation angle of the tilt unit. To this end, we take each network package as sent by the sensor and compute the 6D Euclidean transform for each raw data package based on the IMU-based LiDAR orientation. While the registration of a whole point cloud is a bit more complicated than with the stop-and-go approach, it yields much denser point clouds, as we will show in the next section.

IV. First Experimental Results

As we discussed in the previous section, there are two possible approaches to integrate single point clouds from the LiDAR into a complete local map at the robot's current position. With stop-and-go scanning, we have to compute the 6D Euclidean transform at each tilt angle to register a local map. While scanning, the tilt unit stands still. So, we have to apply the 6D transform for each point cloud as a whole at a certain tilt angle. When scanning continuously, the tilt unit does not come to a stand-still while acquiring data. This means that we need to continuously calculate the

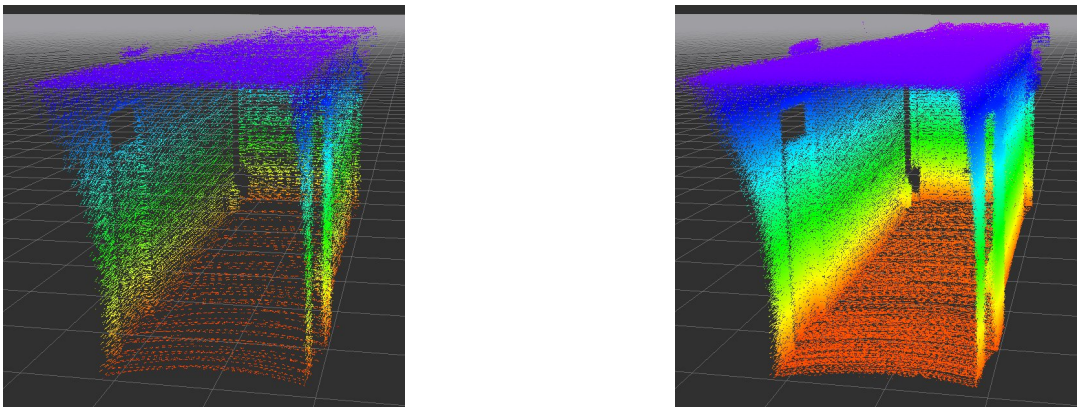

(a) Scan at one position with stop and go tilting (126,650 points)

(b) Scan at one position with continuous tilting (905,748 points)

Figure 6. Comparison between stop-and-go and continuous scanning

6D transforms for each single orientation and tilt angle of the sensor head. The ROS Velodyne driver we developed computes the 6D transform for each network package coming from the LiDAR. As 6×64 single range measurements are gathered in one network package, our transformed point cloud thus has an angular resolution of about $0.5°$ (six times the angular resolution of $0.09°$ provided by the sensor). It is therefore important to get reliable information from the pose of the robot and the orientation of the tilt unit. For acquiring the orientation of the tilt unit, we make use of an AHRS and an IMU. The AHRS is used to compute the orientation and pose of the robot. With an Extended Kalman Filter, we combine the wheel encoder data of the robot with the AHRS orientation data at hand. ROS provides this functionality with the `robot_pose_ekf` package[1]. Data from the wheel encoders, the IMU and the LiDAR are combined based on ROS timestamps. For estimating the relative orientation of the tilt unit, we use an additional IMU sensor which is mounted on the tilt unit. For transforming the incoming LiDAR data in the continuous scan mode, we estimate the orientation of the LiDAR IMU in the following way: at the beginning of a scan we reset the orientation and calculate the initial roll and pitch from gravitational acceleration (e.g. as shown in [23]). For the yaw orientation, we use the yaw angle from the AHRS system. This is the reason why the robot has to stand still when taking a range scan.

Fig. 3 shows some photographs of the setup of the Plabutschtunnel mapping experiment. We teleoperated the robot through the Plabutschtunnel in Graz, Austria, on two days after midnight. One drive lane was closed for tunnel inspection, on the other lane there was still some traffic. Fig. 4 shows range maps from the tunnel portal. The colours indicate the physical height of a measurement. Local maps were acquired roughly every $30\,\mathrm{m}$. The black circles in Fig. 4 and 5 indicate the robot's position in the integrated local map. The black circles stem from a minimal range of about $2\,\mathrm{m}$ around the Velodyne; within this range no reasonable measurements can be taken and displayed. Fig. 5 shows an intensity map of an emergency bay inside the tunnel $1.8\,\mathrm{km}$ away from the tunnel portal. Low reflection intensities are shown in red while high intensities are shown in blue. One can, for one, see the emergency exit tunnel (Fig. 5(c) shows the top view of the emergency exit). For another, one can also see the sign, which was painted on the wall, indicating that the other portal is about $8.4\,\mathrm{km}$ away.

In total, we acquired about 55,000 point clouds of a $2.4\,\mathrm{km}$ stretch of the tunnel during two nights. During these experiments we acquired about 2,5 billion single range measurements. We also compared continuous scanning vs. stop-and-go scanning in this experiment. While it is easier to acquire data with the stop-and-go method, the advantage of scanning continuously is obvious. The acquired point clouds are much denser and, furthermore, the scan time is much lower, as we do not have to stop the motor of the tilt unit in order to take a scan. Denser point clouds allow to reduce outliers and sensor noise from the resulting map in a post-processing step. Usually, a down-sampling step takes place when computing the complete map of the tunnel. With denser point clouds the actual mean of a measurement is approximated better than with sparse data.

While we have to further analyze this in a quantitative fashion, Fig. 6 shows a qualitative result under laboratory conditions. In Fig. 6(a), a point cloud of our institute hallway acquired by stop-and-go is shown. On the right-hand side in Fig. 6(b), the same scene was continuously acquired. Having a closer look at the number of scan and scan points it becomes obvious that continuous scanning leads to more accurate data. In the stop-and-go scan taken in Fig. 6(a), 19 single scans were integrated with a total of 126,650 3D range points acquired with a total scan time of about $116\,\mathrm{s}$. For acquiring the point cloud in Fig. 6(b), about 126 single scans with a total of 905,748 range points were integrated. The scan time lies around $25\,\mathrm{s}$. This is about 7 times as many data than with the stop-and-go scanning method in about $1/4$ of the time. This shows the advantages of continuous scanning. Not only can

[1] http://wiki.ros.org/robot_pose_ekf

more point clouds be acquired during a single sweep, but also the scan time is dramatically reduced. As already mentioned, usually a down-sampling step takes place to further process the data and maps. Here, also the continuous mode is preferable. With denser point clouds, sensor noise and outliers are more likely to be detected and averaged out than with sparse point clouds.

V. Discussion

To achieve the goal of a fully-automated mine, each robot that operates there needs precise 3D maps. On the other hand, sensor equipment just for localizing a robot with an existing high-definition map does not necessarily need to be high-definition. Therefore, it could be cost-effective to just equip one robot with high-definition sensors for mapping, while other robots are using cheaper sensors. With our robot Barney we designed a prototype platform of an underground mapping robot for acquiring dense and precise maps with a high-definition sensor. We showed how we acquire dense point clouds with a HD-LiDAR when tilting it in a continuous fashion. The combination of wheel encoders with the AHRS offers a viable robot odometry which is a good basis for computing accurate 3D maps of underground mines. If we find out in future tests in underground mines that slippage becomes a problem for the odometry, we can, for instance, enhance the odometry using visual odometry or scan matching approaches.

Our future goals are to apply different scan matching algorithms to further improve the alignment of the point clouds taken at a particular position. As the amount of data acquired by the Velodyne is enormous (from our experiments we acquired about 400 GB of point clouds), we will have to down-sample them; this has to be done in a way where not much accuracy is lost. Furthermore, we then want to compare different global matching algorithms on these scans, to get consistent 3D maps. We plan to evaluate the different methods quantitatively with given ground truth data from underground mines. Another improvement for future work might be to use a lighter LiDAR sensor to be able to use simpler and lighter tilt unit designs. This will avoid drawbacks of using an IMU for accurate tilt positions, since a solution with a worm gear creates a backlash that eliminates the possibility of using (exclusive) encoder data. As we have shown, the continuous registration of point clouds is more advantageous than the stop-and-go mapping. In both scenarios, however, the robot stands still when acquiring a local map. In our future work, we also want to map in a continuous-continuous way, i.e. we register scans in the continuous mode while the robot is driving in a constant motion. This would increase the local point cloud density even more.

Acknowledgements

This work was in part supported by the Ministry of Innovation, Science and Research of North-Rhine Westphalia, Germany and by FH Aachen University of Applied Science. We thank K. Krückel, M. Leingartner, J. Maurer and F. Nolden for their support with helping to acquire the data in the Plabutschtunnel. Further, we would like to thank the anonymous reviewers for their helpful comments.

References

[1] E. Lee, "Cyber Physical Systems: Design Challenges," in *Proc. ISORC-08*, 2008, pp. 363–369.
[2] The Economist, "The third industrial revolution," , vol. 12, no. 16, 2012.
[3] D. Kucera, "Amazon Acquires Kiva Systems in Second-Biggest Takeover," 2012, available at http://bloom.bg/Gzo6GU.
[4] IM, "Rapid development for cave mines," *International Mining*, pp. 54–58, 2010, http://www.infomine.com/publications/docs/InternationalMining/Chadwick2010t.pdf.
[5] E. S. Duff, J. M. Roberts, and P. I. Corke, "Automation of an underground mining vehicle using reactive navigation and opportunistic localization," in *Proc. IROS-2003*, vol. 4, 2003, pp. 3775–3780.
[6] J. M. Roberts, E. S. Duff, P. I. Corke, P. Sikka, G. J. Winstanley, and J. Cunningham, "Autonomous control of underground mining vehicles using reactive navigation," in *Proc. ICRA-00*, vol. 4. IEEE, 2000, pp. 3790–3795.
[7] S. Scheding, G. Dissanayake, E. M. Nebot, and H. Durrant-Whyte, "An experiment in autonomous navigation of an underground mining vehicle," *IEEE Transactions on Robotics and Automation*, vol. 15, no. 1, pp. 85–95, 1999.
[8] E. M. Nebot, "Surface mining: main research issues for autonomous operations," in *Robotics Research*. Springer, 2007, pp. 268–280.
[9] J. Green, P. Bosscha, L. Candy, K. Hlophe, S. Coetzee, and S. Brink, "Can a robot improve mine safety?" in *Proceedings of the 25th International Conference of CAD/CAM, Robotics & Factories of the Future Conference*, 2010.
[10] J. Dickens and R. Teleka, "Mine safety sensors: Test results in a simulated test stope," in *Proc. RobMech-2013*, 2013, pp. 105–110.
[11] A. Chikwanha, S. Motepe, and R. Stopforth, "Survey and requirements for search and rescue ground and air vehicles for mining applications," in *Proc. M2VIP-12*, 2012, pp. 105–109.
[12] M. Buehler, K. Iagnemma, and S. Singh, Eds., *The DARPA Urban Challenge: Autonomous Vehicles in City Traffic*, ser. Springer Tracts in Advanced Robotics,. Springer, 2010, vol. 56.
[13] P. J. Besl and N. D. McKay, "A method for registration of 3-d shapes," *IEEE Trans. Pattern Anal. Mach. Intell.*, vol. 14, no. 2, pp. 239–256, 1992.
[14] S. Thrun, S. Thayer, W. Whittaker, C. Baker, W. Burgard, D. Ferguson, D. Hahnel, D. Montemerlo, A. Morris, Z. Omohundro, C. Reverte, and W. W, "Autonomous exploration and mapping of abandoned mines," *IEEE Robot. Autom. Mag.*, vol. 11, no. 4, pp. 79–91, 2004.
[15] C. Baker, Z. Omohundro, S. Thayer, W. Whittaker, M. Montemerlo, and S. Thrun, "A case study in robotic mapping of abandoned mines," in *Field and Service Robotics*, ser. Springer Tracts in Advanced Robotics. Springer Berlin / Heidelberg, 2006, vol. 24, pp. 487–495.
[16] A. Nüchter, K. Lingemann, J. Hertzberg, and H. Surmann, "6d slam-3d mapping outdoor environments: Research articles," *J. Field Robot.*, vol. 24, no. 8-9, pp. 699–722, 2007.
[17] A. Nüchter, *3D Robotic Mapping - The Simultaneous Localization and Mapping Problem with Six Degrees of Freedom*, ser. Springer Tracts in Advanced Robotics. Springer, 2009, vol. 52.
[18] A. Morris, D. Ferguson, Z. Omohundro, D. Bradley, D. Silver, C. Baker, S. Thayer, C. Whittaker, and W. Whittaker, "Recent developments in subterranean robotics," *J.Field Robot.*, vol. 23, no. 1, pp. 35–57, 2006.
[19] Z. Taylor and J. Nieto, "Automatic calibration of lidar and camera images using normalized mutual information," in *Proc. ICRA-13*, 2013.
[20] M. Quigley, K. Conley, B. P. Gerkey, J. Faust, T. Foote, J. Leibs, R. Wheeler, and A. Y. Ng, "Ros: an open-source robot operating system," in *ICRA Workshop on Open Source Software*, 2009.
[21] http://commons.wikimedia.org/wiki/File:Plabutschtunnel-S%C3%BCd.JPG, last visited: Nov, 10, 2014.
[22] R. B. Rusu and S. Cousins, "3d is here: Point cloud library (pcl)," in *Proc. ICRA-11*. IEEE, 2011.
[23] X. Yun, E. R. Bachmann, and R. B. McGhee, "A simplified quaternion-based algorithm for orientation estimation from earth gravity and magnetic field measurements," *IEEE T. Instrumentation and Measurement*, pp. 638–650, 2008.